Out-of-plane optical transmittance
of 2D photonic macroporous silicon structures

L.A. Karachevtseva, A.E. Glushko, V.I. Ivanov, O.O. Lytvynenko,
V.F. Onishchenko, K.A. Parshin, O.J. Stronska
V. Lashkaryov Institute of Semiconductor Physics, NAS of Ukraine, 45, prospect Nauky, 03028 Kyiv, Ukraine
Phone: 525 9815, fax: 525 8243, e-mail: lakar@isp.kiev.ua

Abstract. Optical transmission spectra of 2D photonic macroporous silicon structures are investigated. The absolute bandgap for high values of the out-of-plane component k_z is situated between the second and third photonic bands. Essential reduction in the transmittance of electromagnetic radiation and the step formation are observed for wavelengths less than the optical period of structures due to directed and decay optical modes formed by macroporous silicon as a short waveguide. The absorption in the macroporous silicon structure is determined by a maximum of the longitudinal component of electromagnetic waves, its interaction with 2D surface oscillations, and the appearance of polaritonic resonances.

1. Introduction

Macroporous silicon can be considered as an ideal 2D and 3D photonic crystal due to high aspect ratios of macropores and a periodic variation of the photoelectrochemical etching parameters [1-3]. The lattice constants can be varied in the range from 8000 down to 500 nm, resulting in complete bandgaps in a wavelength range between 20 and 1.3 μm. Point defects, 3D photonic crystals, microchips in a photonic crystal based on macroporous silicon were characterized in [4-10]. Sharp resonances were recorded in the bandgap of photonic crystals with defects, in excellent agreement with the results of numerical simulations by applying a tight-binding model [4, 5]. Extended 3D photonic crystals based on macroporous silicon are prepared due to a periodic variation of the illumination during photoelectrochemical etching [6] and subsequent focused-ion-beam drilling [7]. All-optical transistor action in photonic bandgap silicon materials doped with active atoms was described in [8]. The concept of a hybrid 2D-3D photonic bandgap silicon heterostructure, which enables the planar light-wave propagation in engineered wavelength-scale microcircuits, was introduced in [9]. The incorporation of semiconductor quantum dots as internal emitters into 2D photonic crystals of macroporous silicon was reported in [10]. In addition, a spectral modification of the emission by the surrounding photonic crystal was demonstrated for mercury telluride quantum dots, when the emission coincides with the photonic bandgap of the silicon photonic crystal.

Diffraction efficiency, birefringence, and polaritonic and structural gaps on the silicon-based photonic crystals were studied in [11-13]. A 2D photonic crystal can exhibit spectral regions of very small diffraction efficiency [11], while the diffraction efficiency is near unity in other regions. The experimental results agree well with the corresponding numerical calculations and highlight the prominent role of the surface termination, an aspect which cannot be described by the photonic band structure alone. Such additional spectral filters have possible applications in Raman and photoluminescence spectroscopy. The experimental and theoretical studies of the birefringence of two-dimensional silicon photonic crystals in the spectral region below the first photonic bandgap were reported in [12]. The measured birefringence was defined as the difference in the effective refractive indices of the electric fields polarized in parallel and perpendicularly to the cylinder axis and reached a maximum value of 0.366 near the first photonic band edge. The results demonstrate the potential use of two-dimensional photonic crystals for highly birefringent optically integrated devices. The coexistence and interaction of polaritonic and structural gaps are studied in [13] on one-dimensional photonic crystals Si/SiO_2, SiO_2/Si, and SiO_2/air. The calculated results verify the

presence of a polaritonic gap in photonic crystals Si/SiO$_2$ for thicknesses much lower than the wavelength for the cases SiO$_2$/Si and SiO$_2$/air.

Theoretical and experimental results obtained during last years demonstrate the potential use of silicon-based photonic crystals for active and passive optically integrated devices [14]. 2D photonic crystals on the basis of macroporous silicon are perspective for use in the infrared range of electromagnetic waves due to the effective transformation of a spectrum of electromagnetic radiation. The presence of periodically located cylindrical pores divided by silicon columns provides the big effective surface of a sample which determines the optical and electrophysical characteristics of macroporous silicon structures [15]. In this paper, the out-of-plane optical transmission spectra of 2D photonic macroporous silicon structures have been investigated with the purpose of a definition of new opportunities for applications of such structures. The incidence direction of electromagnetic radiation in parallel to macropores is more technological for planar technologies. The basic researches of optical characteristics have been concentrated also on this variant. The dependences of photoconductivity and Raman scattering on the angle of incidence of the electromagnetic radiation were observed by taking into account the comparative analysis of a surface of

macroporous silicon by methods of electron microscopy, infrared absorption, and the modulation spectroscopy of electroreflection

2. Methodology

The starting material consisted of *n*-type silicon (100) with a resistivity of 4.5 Ohm·cm. Macropores were formed with diameters $D_p = 1$-$10\ \mu$m due to the generation and transfer of nonequilibrium holes to the *n*-Si electrochemically treated surface as a result of the optical band-to-band electron-hole generation [16]. Periodic structures as well as structures with arbitrary distribution of macropores have been fabricated (Fig. 1a and b). Optical transmittance was measured using an IR Fourier spectrometer IFS-113 and an IR spectro-photometer Specord M85.

3.Results

3.1. Photonic bandgap

For the out-of-plane light propagation, a sharp increase in absorption and the photonic bandgap formation is observed at wavelengths between one and two optical periods $\lambda_a < \lambda < 2\lambda_a$ of the macroporous silicon structure (λ_a is equal to $(a - D_p)\varepsilon^{1/2} + D_p$); *a* –the structure period, and D_p – the diameter of macropores). Thus, the absolute
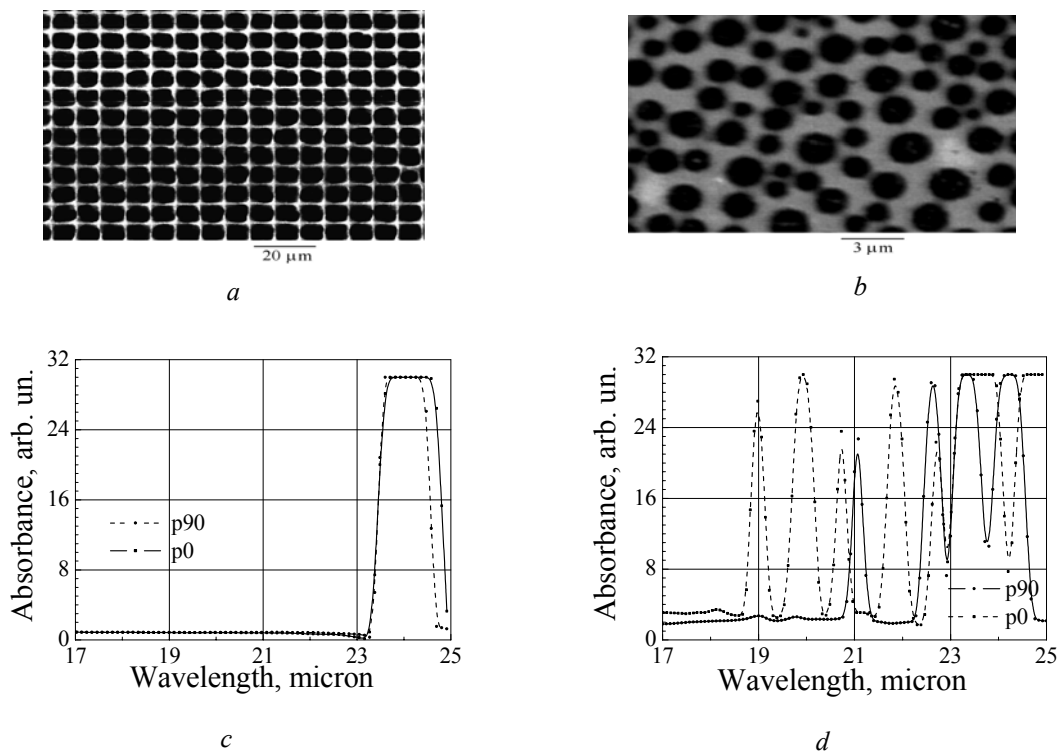

Fig. 1. Periodic (a) and arbitrary (b) macroporous silicon structures. Optical absorption of electromagnetic waves propagated in periodic (c) and arbitrary (d) macroporous silicon.

photonic bandgap was measured for the light direction parallel to macropores for planar technologies at $\lambda = 1.2-1.5\lambda_a$. One photonic bandgap is formed for periodic structures (Fig. 1c), and the narrow peaks of the density of states are formed for the structure with arbitrary macropore distribution (Fig. 1d).

Optical transmittance of 2D periodic structures was investigated for the out-of-plane direction in [17, 18]. Within the plane-wave method, Maradudin and McGurn in [17] had calculated the dispersion curves of electromagnetic wave propagation in a two-dimensional periodic structure. The structure studied numerically possesses a bandgap between 3 and 4 zones common to waves of both E- and H-polarizations propagating in the plane parallel to the rods. In [18], the transmission of electromagnetic waves propagating in 2D photonic crystals for the out-of-plane incident angle as high as 85° was studied. There is a full calculated photonic bandgap for both E- and H-polarizations for the ratio of dielectric constants higher than 12.25. Our calculations of the out-of-plane propagation of electromagnetic waves through a square-lattice photonic crystal by the plane-wave method show that the absolute bandgap appears for high values of the out-of-plane component k_z. In our case, the bandgap opens up for $k_z a > 4.5$ and is situated between the second and third bands (Fig. 2). As it obvious, the gap width increases and its edges shift sufficiently to higher frequencies. Our experimental results (Fig. 1c) correspond to $k_z a = 5$ and $\omega a / 2\pi c = 0.32-0.35$.

3.2. Polaritonic absorption band

Absorption spectra of macroporous silicon with different macropore diameters and concentrations have common features at $\lambda \leq \lambda_a$ (Fig. 3). There is an essential reduction in the transmittance of electromagnetic radiation as the wavelength shortens [15]. At short wavelengths, $\lambda < D_p$, (Fig. 3, curve 1) and at wavelengths $\lambda < (a - D_p) n_{Si}$
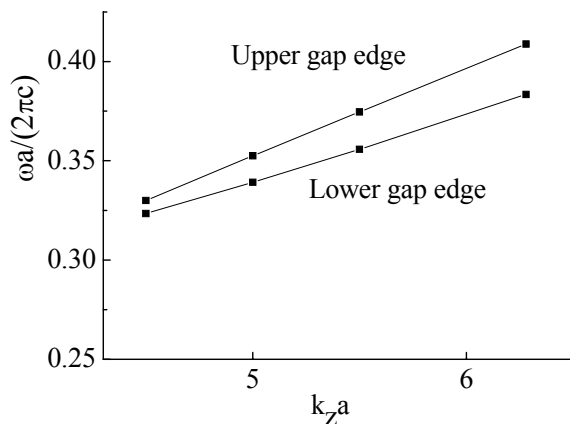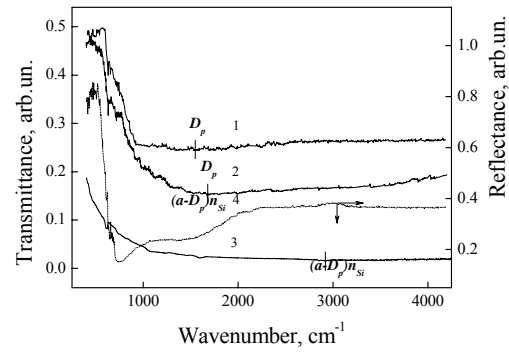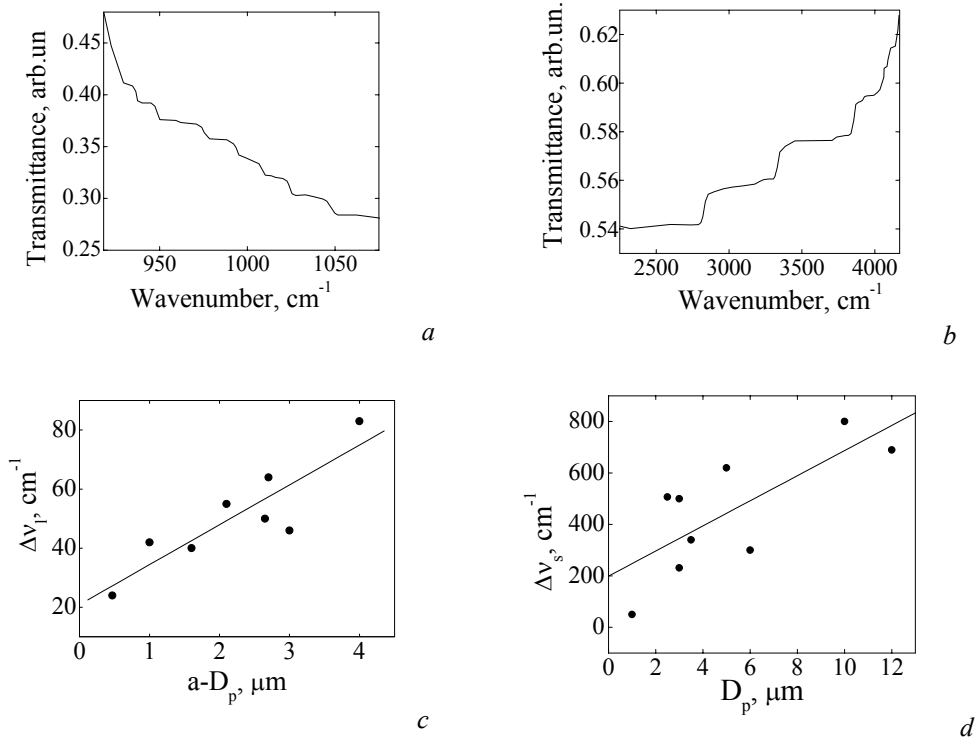

Fig. 3. Transmittance spectra of macroporous silicon structures with parameters: $1 - D_p > (a - D_p) n_{Si}$; $2 - D_p \approx (a - D_p) n_{Si}$; $3 - D_p < (a - D_p) n_{Si}$; reflectance spectra of monocristalline silicon (4).

(Fig. 3, curves 2, 3), the optical transmittance grows slightly. The area of the maximal absorption of this band depends on the difference of the macropore diameter D_p and distances between pores, $a - D_p$. The maximal absorption is measured in an interval of frequencies $[(a - D_p)n_{Si}]^{-1} > \nu > (D_p)^{-1}$ at $D_p > (a - D_p)n_{Si}$ (curve 1) and in an interval of frequencies $[(a - D_p)n_{Si}]^{-1} < \nu < (D_p)^{-1}$ for $D_p < (a - D_p)n_{Si}$ (curve 3). Structures with a macropore diameter comparable to the distance between pores $D_p \sim (a - D_p)n_{Si}$ have the transmission minimum at $\nu = [(a - D_p)n_{Si}]^{-1} \cong (D_p)^{-1}$ (curve 2). In the first case, the long-wave band edge is measured up to the frequencies of transverse optical phonons (520 cm^{-1}) that is correlated with a reflection growth for single-crystal silicon (Fig. 3, curve 4) due to the lattice absorption in the silicon matrix. The transmission reduction with decrease in the lattice absorption testifies that the phonon modes "extinguish" the mechanism of electromagnetic energy dissipation in macroporous silicon structures.

The transmission spectra (Fig. 3) contain steps or oscillations, as in Fig. 4. The step frequency in the long-wave part of the spectrum is proportional to the distance between pores ($\Delta \nu^l \sim a - D_p$). But, in the short-wave region, it is proportional to the diameter of pores ($\Delta \nu^s \sim D_p$). The transmission spectra of macroporous silicon as well as the formation of the steps can be explained by a model of directed and decay optical modes in macroporous silicon as a short waveguide structure [19, 20]. In the short-wave spectral region, the directed optical modes are formed on macropores, because the step growth of transmittance takes place for $\lambda \leq D_p$ (Fig. 4). In the middle region $D_p < \lambda < \lambda_a$, the formation of the directed mode for silicon waveguides and the decay mode for macropores is possible. Such modes are formed in the same medium (the silicon matrix) and differ by the sign of the radius ρ only (Table). The amplitude of the total wave in the direction

Fig. 2. The dependence of the bandgap edge position on the k_z component.

Table. Mode characteristics in macroporous silicon structures as in [19].

	Region	Propagation constant, β	Mode parameter
Directed optical modes	Macropore	$k\cos\theta_z$, $0 < \beta < k$	$U_p = k\rho\,(1 - \cos\vartheta_z^2)^{1/2}$
	Silicon matrix	$kn_{Si}\cos\theta_z$, $k < \beta < kn_{Si}$	$U_{Si} = k\rho_{Si}\,n_{Si}\,(1 - \cos\vartheta_z^2)^{1/2}$
Polaritonic modes	Macropore	$-ik\,n_{Si}\cos\theta_z$, $k^2 < |\beta|^2 < (kn_{Si})^2$	$W_p = k\rho\,n_{Si}\,(1 - \cos\vartheta_z^2)^{1/2}$
	Silicon matrix	$-ik\cos\theta_z$, $0 < \beta < k$	$Q_{Si} = ik\rho_{Si}\,(\cos\vartheta_z^2 - 1)^{1/2}$

Fig. 4. Long-wave steps in the transmittance spectrum (a), short-wave steps in the transmittance spectrum of macroporous silicon (b), dependence of the long-wave step frequency $\Delta\nu_l$ on the distance between pores $a-D_p$ (c), dependence of the short-wave step frequency $\Delta\nu_s$ on the pore diameter D_p (d).

z is defined by the cylindrical functions $J_n^{Si}(Q)e^{i\beta z} + I_n^p(-Q)e^{-\beta z}$. In the long-wave spectral region $\lambda > \lambda_a$, the decay modes are formed in the silicon matrix with the mode parameter $Q_{Si} = ik\rho_{Si}\,n_{Si}(\cos\vartheta z^2 - 1)^{1/2}$. The increase in the diameter of macropores up to $D_p > (a - D_p)n_{Si}$ modifies the transmission spectrum. In this case, the region of the directed mode formation corresponds to $\lambda < a - D_p$ and the decay modes are formed for $\lambda > D_p$.

Transmission spectra of macroporous silicon structures were measured by a spectrophotometer with an aperture of about 10°. Therefore, under the

formation of the optical mode, the multimode regime should be realized. However, the step formation testifies to the realization of the one-mode regime that is related to surface oscillator fluctuations on the macropore surface and with the surface polariton formation. This is supported by the preferable absorption of the *p*-components of the electromagnetic radiation incident on macroporous silicon structures (Fig. 5). In addition, the excitation of a surface electromagnetic wave is accompanied by a reduction in the reflected light intensity and an increase in the absorption.
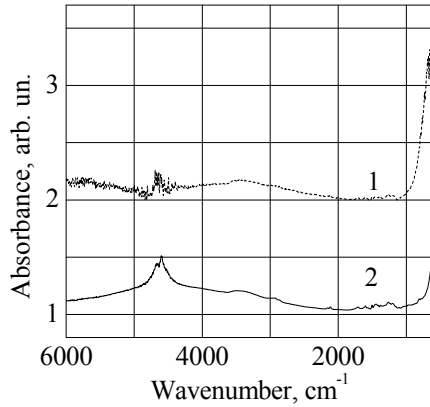
Fig. 5. Absorption spectra of the *p*-component (1) and *s*-component (2) of the electromagnetic radiation incident on macroporous silicon.

4. Discussion

Absorption of macroporous silicon at $\lambda \le \lambda_a$ is determined by the longitudinal component of electromagnetic waves in macroporous silicon structure as a short waveguide with specific surface (Fig. 3). The comparative analysis of the surface of macroporous silicon by methods of electron microscopy, infrared absorption, and modulation spectroscopy of electroreflection was carried out in [20-22]. It was established that the microstructure, local center structure, and built-in electric field on a macropore surface essentially depend on parameters of the electrochemical process, that is, on the initial voltage and the current density. The periodic oscillation in electroreflection spectra (Franz-Keldysh's effect) and the effect of increase in the built-in electric field were measured due to a positive charge built in the oxide layer on the macropore walls. The electric field intensity F_s on a macropore surface varies from $4 \cdot 10^5$ to $9 \cdot 10^5$ V/cm [21]. The value of the built-in field on a cylindrical macropore is defined by the surface concentration of Si-O and Si-H bonds [22]. In addition, the sign of the main maximum in the spectra of electroreflectance and the dependence of its magnitude on a constant voltage [21] correspond to the formation of an inversion layer on the macropore surface. Franz-Keldysh oscillations are a result of the triangular potential barrier on a macropore surface and determine two-dimensional surface carrier oscillations. Thus, the longitudinal component of electromagnetic waves in the macroporous silicon structure interacts effectively with surface oscillators, and polaritonic resonances in absorption are observed.

In addition, the photoconductivity of macroporous silicon structure depends on an incidence angle of electromagnetic radiation (Fig. 6). For periodic structures, maxima of photoconductivity are formed (1) at the normal incidence of electromagnetic radiation, (2) in the region of the angle of total internal reflection with

respect to the macropore walls, and (3) for the grazing incidence of light with respect to the structure surface [23]. At the angles of incident light close to normal ones, the directed optical modes (Fig. 3) are localized on macropores. At the angle of total internal reflection with respect to the macropore walls, the surface TM-wave propagating along macropores is formed. At the angles of incidence close to grazing ones, the periodic relief of the structure transforms the incident light wave into a surface one as a result of the *m*-order diffraction. Thus, the photoconductivity maximum corresponds to a maximum of the longitudinal component of electromagnetic waves in analogy to light absorption.

The effect of the enhancement of Raman scattering in the photonic structures of macroporous silicon was measured in [24]. The band position in spectra coincides with the position of the band for single-crystal silicon, but its intensity strongly depends on the macropore size and the light incidence angle. The maximal scattering intensity was registered for the samples with the minimal diameter of pores (about 1 μm) at an incidence angle of 25-30 degrees (Fig. 6). This maximum corresponds to the angle of total internal reflection with respect to the macropore walls, when the longitudinal component of electromagnetic waves is maximal. The mechanism of Raman scattering enhancement is determined by the surface electromagnetic mode formation and the scattering on it. Thus, the photoconductivity and Raman scattering maxima are determined by the corresponding maximum of the longitudinal component of electromagnetic waves in the macroporous silicon structure in analogy to light absorption.

The cylinder consisting of a substance with frequency-dependent dielectric permeability ($l = 1$) possesses dispersive frequencies in a plane perpendicular to the cylinder axis which satisfy the relation [25]:

$$\Omega_\mu^2(q) = \omega_p^2 \{[\varepsilon_\infty - \varepsilon_1 I_\mu(\xi) \ K_\mu'(\xi)/J_\mu'(\xi)K_\mu(\xi)]\}^{-1}. \quad (1)$$

where $I_\mu(\xi)$ and $K_\mu(\xi)$ are the μ-order cylindrical Bessel functions; ξ, q, and p are the parameters of a mode determined by the optical mode modulated by surface oscillator fluctuations. In this case, the surface polariton frequency is the lower surface plasmon frequency ω_p, and frequency-dependent dielectric permeability grows $\Delta\varepsilon(\omega) > 0$. In the opposite case (the cylinder with constant dielectric permeability is placed in a material with frequency dispersion in the region of surface polariton frequencies, $l = 2$), we have:

$$\Omega_\mu^2(q) = \omega_p^2 \{\varepsilon_\infty - \varepsilon_1 I_\mu'(\xi)K_\mu(\xi)/J_\mu(\xi)K_\mu'(\xi)]\}^{-1}. \quad (2)$$

The dependences of the resulted dispersive frequencies on the mode parameter ξ are presented in Fig. 7. The dependence of the surface plasmon frequency on ξ is essential for zero-order modes at $\xi < 3$. The dispersion law has the classical form for $\xi > 3$:

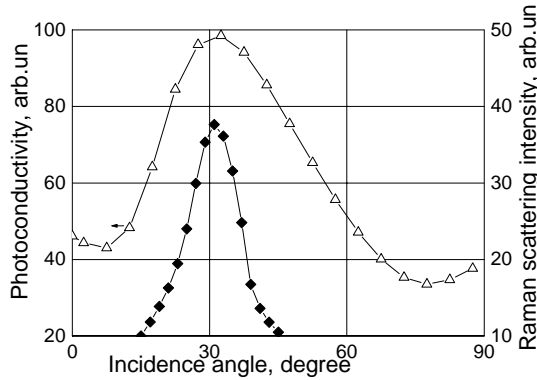$$\Omega_\mu^2(q) = \omega_p^2 (\varepsilon_\infty + \varepsilon_1)^{-1}. \quad (3)$$

Fig. 6. Photoconductivity (Δ) and Raman scattering ($\blacklozenge$) of the macroporous silicon structure versus the light incidence angle.
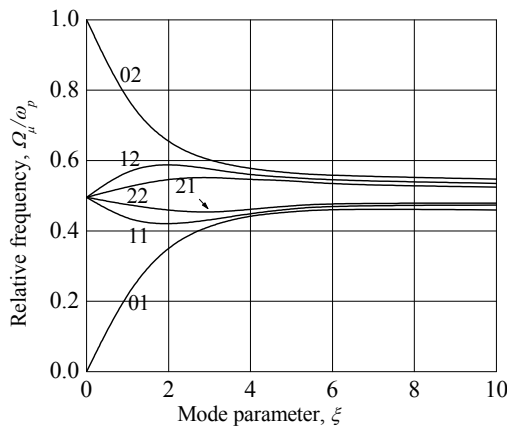

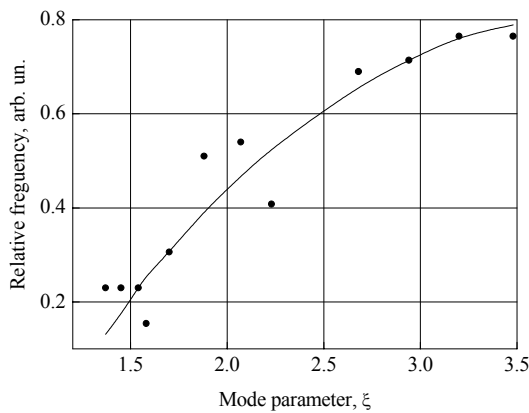**Fig. 7.** Dependences of frequencies on the mode parameter ξ for $\mu = 0, 1, 2$ and $l = 1, 2$.

Fig. 8. Experimental dependence of relative frequency $2\pi c\Delta\nu_s/\Omega_\mu$ versus mode parameter ξ.

The dispersion law of a surface plasmon for $k >> \Omega_\mu /c$ is determined by the root dependence [26],

$$\Omega_\mu = [k\omega_p c(\varepsilon_\infty + \varepsilon_1)^{-1}]^{1/2}; \qquad (4)$$

The experimental dependence of the relative frequency $2\pi c\Delta\nu_s/\Omega_\mu$ on the mode parameter ξ is shown in Fig. 8. The frequency growth is observed with increase in the wave vector according to relations (3) and (4). Thus, the dispersion law of polaritonic modes in macroporous silicon structures is determined by the root dependence $\Omega_\mu \sim (k)^{1/2}$ for optical modes of zero order at the mode parameter $\xi < 3$.

5. Conclusions

Out-of-plane optical transmission spectra of 2D photonic macroporous silicon structures are investigated. The absolute bandgap for high values of the out-of-plane component k_z is situated between the second and third bands at $k_za = 5$ and $\omega a /2\pi c = 0.32\text{-}0.35$. The theoretically unpredicted reduction in the transmittance of electromagnetic radiation and the step formation are observed for wavelengths less than the optical period of transmission of the structures due to the directed and decay optical modes formed by macroporous silicon as a short waveguide structure. The absorption maximum corresponds to the directed optical mode formation. The prevalence of absorption over reflection of light testifies to the polaritonic type band formation. Surface polaritons are formed on decay modes at the formation of directed optical modes on a macropore or the silicon matrix.

The comparative analysis of the surface of macroporous silicon by methods of electron microscopy, infrared absorption, and modulation spectroscopy of electroreflection is carried out. Electroreflectance spectroscopy of the macroporous silicon surface showed the presence of the intrinsic electric field near 10^6 V/cm due to a positive charge built in the oxide layer on the macropore walls. Franz–Keldysh oscillations confirm the triangular surface barrier formation that results in two-dimensional surface carrier oscillations. Thus, the longitudinal component of electromagnetic waves in the macroporous silicon structure interacts effectively with surface oscillators, and polaritonic resonances in absorption, photoconductivity, and Raman scattering are manifested and have been measured. The dispersion law of polaritonic modes is determined by the root dependence $\Omega_\mu \sim (k)^{1/2}$ for optical modes of zero order at the mode parameter $\xi < 3$.

We believe that devices on the base of 2D photonic macroporous silicon structures will meet a variety of applications in view of integrated nanophotonic circuits. The photosensitivity enhancement and the polaritonic mode formation will inspire the development of active and passive elements in photonic crystal microchips and compact highly sensitive uncooled detectors of light radiation.

Acknowledgements

References

1. A. Birner, R. Wehrspohn, U. Gösele, K. Busch, Silicon-based photonic crystals // *Adv. Mater.* **13**(6), p. 377-388 (2001).

2. J. Schilling, R.B. Wehrspohn, A.Birner, *et al.*, A model system for two-dimensional and three-dimensional photonic crystals: macroporous silicon // *J. Opt. A: Pure Appl. Opt.* **3,** p. S121–S132 (2001).

3. R. Hillebrand, C. Jamois, J. Schilling, R.B. Wehrspohn, W. Hergert, Computation of optical properties of Si-based photonic crystals with varying pore diameters // *Phys. status solidi* (*b*) **240**(1), p. 124-133 (2003).

4. P. Kramper, A. Birner, M. Agio *et al.*, Direct spectroscopy of a deep two-dimensional photonic crystal microresonator // *Phys. Rev. B* **64**(23), 233102 (2001).

5. Stefan Richter, Reinald Hillebrand, Cecile Jamois, *et al.*, Periodically arranged point defects in two-dimensional photonic crystals // *Phys. Rev. B* **70**(19), 193302 (2004).

6. J. Schilling, F. Müller, R.B. Wehrspohn, U. Gösele, K. Busch, Dispersion relation of 3D photonic crystals based on macroporous silicon // *Mat. Res. Soc. Symp. Proc.* **722,** p. L6.8 (2002).

7. J. Schilling, J. White, A. Scherer, G. Stupian, R. Hillebrand, U. Gösele, Three-dimensional macroporous silicon photonic crystal with large photonic band gap // *Appl. Phys. Lett.* **86,** 011101 (2005).

8. John Sajeev, Marian Florescu, Photonic bandgap materials: towards an all-optical micro-transistor // *J. Opt. A: Pure Appl. Opt.* **3**(6), p. S103–S120 (2001).

9. Chutinan Alongkarn, John Sajeev, Toader Ovidiu, Diffractionless flow of light in all-optical microchips // *Phys. Rev. Lett.* **90**(12), 123901 (2003).

10. S. Richter, M. Steinhart, H. Hofmeister *et al.*, Quantum dot emitters in two-dimensional photonic crystals of macroporous silicon // *Appl. Phys. Lett.* **87**, 142107 (2005).

11. F. Müller, A. Birner, U. Gösele, V. Lehmann, S. Ottow, H. Föll, Structuring of macroporous silicon for applications as photonic crystals // *Journal of Porous Materials* **7**(1-3), p. 201-204 (2000).

12. F. Genereux, S.W. Leonard, H.M. van Driel, A. Birner, U. Gösele, Large birefringence in two-dimensional silicon photonic crystals // *Phys. Rev. B* **63**(16), 161101 (2001).

13. Herman Högström, Carl G. Ribbing. Polaritonic and photonic gaps in SiO_2/Si and SiO_2/air periodic structures // *Photonics and Nanostructures – Fundamentals and Applications* **2**(1), p. 23-32 (2004).

14. L.A. Karachevtseva, Two-dimensional photonic crystals as perspective materials of modern nanoelectronics // *Semiconductor Physics, Quantum Electronics & Optoelectronics* **7**(4), p. 430-435 (2004).

15. L.A. Karachevtseva, O.A. Litvinenko, E.A. Malovichko, E.I. Stronska, Optical transmittance of 2D macroporous silicon structures // *Semiconductor Physics, Quantum Electronics & Optoelectronics* **4**(4), p. 347-351 (2001).

16. L.A. Karachevtseva, O.A. Lytvynenko, E.J. Stronska, Development and optical characteristics of the macroporous silicon structures // *Semiconductor Physics, Quantum Electronics & Optoelectronics* **3**(1), p. 22-25 (2000).

17. A.A. Maradudin, A.R. McGurn, Out-of-plane propagation of electromagnetic waves in a two-dimensional periodic dielectric medium // *J. Mod. Opt.* **41**(2), p. 275-284 (1994).

18. M.M. Sigalas, R. Bismas, K.M. Ho, and C.M. Soukoulis, Theoretical investigation off-plane propagation of electromagnetic waves in two-dimensonal photonic crystals // *Phys. Rev. B* **58**(11), p. 6791-6794 (1998).

19. A.W. Snyder, J.D. Love, *Optical Waveguide Theory*. Charman and Hall, London, New York, 1983.

20. S. Solimeno, B. Crosignani, P. DiPorto, *Guiding, diffraction and confinement of optical radiation*. Academic Press, New York, 1986.

21. L.A. Karachevtseva, O.A. Lytvynenko, Y. Fukuda, K. Furuya, Photoluminescence of complex microporous-macroporous silicon structures // *Fifth Intern. Confer. on Material Science and Material Properties for Infrared Optoelectronics, Proc. SPIE* **4355,** p. 146-154 (2001).

22. R.Yu. Holiney, L.A. Matveeva, E.F. Venger, O.A. Litvinenko, L.A. Karachevtseva. Electroreflectance study of macroporous silicon surfaces // *Appl. Surface Sci.* **172**(3), p. 214-219 (2001).

23. L.A. Karachevtseva, O.A. Litvinenko, E.I. Stronskaya, Investigation of the local chemical states in the structures of macroporous silicon // *Theoretical and Experimental Chemistry* **39**(2), p. 85-89 (2003).

24. L.A. Karachevtseva, N.I. Karas', V.F. Onischenko, F.F.Sizov, Surface polaritons in 2D macroporous silicon structures // *International Journal of Nanotechnology* **3**(1), p. 76-88 (2006).

25. O.P. Burmistrova, V.A. Kosobukin, Radiative decay of surface collective exitations in polarizable cylinders // *Phys. status solidi* (*b*) **112,** p. 675-683 (1982).

26. M.I. Dmitruk, V.G. Litovchenko, V.L. Strizshevsky, *Surface Polaritons in Semiconductors and Dielectrics*. Naukova Dumka, Kyiv, 1989 (in Russian).